Opt Quant Electron (2007) 39:927–937
DOI 10.1007/s11082-007-9159-4

Mathematical analysis of the lasing eigenvalue problem for the optical modes in a layered dielectric cavity with a quantum well and distributed Bragg reflectors

Volodymyr O. Byelobrov · Alexander I. Nosich

Received: 19 July 2007 / Accepted: 20 November 2007 / Published online: 25 December 2007
© Springer Science+Business Media, LLC. 2007

Abstract Optical modes and associated linear threshold values of material gain bringing them to lasing are investigated for a VCSEL-type cavity with a quantum well, sandwiched between two distributed Bragg reflectors. They are found as solutions to a specific novel eigenvalue problem with the "active" imaginary part of the quantum well refractive index. For the calculation of the Bragg mirror reflection coefficients, well-established method of the transfer matrices is used. The presented results accurately quantify intuitively predictable lowering of the modal thresholds for the modes whose lasing frequencies lay inside the reflectors rejection bands. Besides, they demonstrate that this approach automatically incorporates the account of overlapping between the active region and the modal E-field patterns and its effect on the thresholds.

Keywords Bragg reflector · Eigenproblem · Laser · Microcavity · Threshold · Transfer matrix · VCSEL

1 Introduction

Modern etching and epitaxial technologies operate mostly with flat material layers and enable well-controlled fabrication of multilayered heterostructures. Thin active regions shaped as quantum wells (QWs) or layers of random quantum dots and embedded in epitaxially grown semiconductor microresonators are widely used in photonics. The area of applications of such active cavities covers fundamental aspects such as alteration of spontaneous emission characteristics in various systems and visualization of quantum optical phenomena, and also device applications such as fabrication of vertical cavity surface emitting lasers (VCSELs) (Yu 2003; Piprek 2005; Streiff et al. 2003; Yang et al. 1995; Huffaker and Deppe 1997; Klein et al. 1998; Noble et al. 1998; Chung et al. 2004; Zhang et al. 2006; De Leonardis et al. 2007), microdisk lasers, and photonic-crystal membrane band-edge lasers (Campenhout et al. 2005).

V. O. Byelobrov (✉) · A. I. Nosich
Institute of Radiophysics and Electronics NASU, ul. Proskury 12, Kharkiv 61085, Ukraine
e-mail: volodia.byelobrov@gmail.com

For example, in a VCSEL-type light-emitting device high-intensity optical field is usually confined by the top and bottom distributed Bragg reflectors (DBRs) composed of the quarter-wavelength multilayers grouped in periodic pairs, and a few nanometer wide QW is located inside a half-wavelength or wider cavity layer.

As known, there are several important physical mechanisms responsible for the lasing in microcavities: transport of carriers, heating, and optical confinement, coupled together in non-linear manner (Streiff et al. 2003). Accurate account of all of them is a hard task, and a useful reduction of complexity is achieved through neglecting all non-electromagnetic effects and viewing the optical field as a solution to the linear set of source-free Maxwell equations.

Until recently, such a linear modelling of microcavity lasers has implied exclusively the calculation of the natural modes of the "cold" or, equivalently, *passive* open dielectric resonators. Mathematically this means solving the time-harmonic Maxwell eigenvalue problem with the outgoing-wave radiation condition at infinity for the complex-valued natural frequencies or wavenumbers, k. Such eigenvalues form a *discrete* set and can be numbered, say, by using the index n. In these analyses, the modes with the largest Q-factors have been identified as the lasing modes (Yang et al. 1995; Huffaker and Deppe 1997; Klein et al. 1998; Noble et al. 1998; Chung et al. 2004; Zhang et al. 2006; De Leonardis et al. 2007). The eigenfunctions corresponding to these eigenvalues are the natural electromagnetic fields of the cavity; they decay in time as $\mathrm{e}^{-|\mathrm{Im}\, k_n|ct}$ however grow in space as $\mathrm{e}^{|\mathrm{Im}\, k_n|R}$ far from the cavity (c is the light velocity).

In general, cold-cavity modelling has proved to be an adequate way for predicting the frequency of lasing, which is determined mainly by the cavity shape together with its size and material and lies within the photoluminescence band of the bulk QW material system. However, whilst being meaningful and useful modelling of laser as a cold cavity has very important drawback. The lasing phenomenon is not addressed directly through the Q-factor—neither the presence of active region nor the specific value of material gain that is needed to force a mode to become lasing is included in the formulation. Therefore direct quantification of lasing thresholds and their dependence on the microcavity, QW and DBRs geometry and composition has not been realized yet. For example, the threshold current for the onset of lasing is known to be very sensitive to the location and size of current-injection electrodes. It is also experimentally known that, in order to achieve ultralow room-temperature thresholds, a good overlap between the active region location and width and the cavity natural-mode field is important. The mentioned features have still to be incorporated into the linear electromagnetic model of the laser.

To determine the threshold of lasing, "hot" laser models dwell on the use of the rate equations and involve complicated non-linear descriptions (Yu 2003; Piprek 2005; Streiff et al. 2003). Unlike the mentioned studies, in this work we report the results of the direct quantification of the lasing spectra and associated thresholds of the modes in a laterally uniform, i.e., one-dimensional (1D) model of the VCSEL-type layered microcavity equipped with a QW by using a specifically tailored linear eigenvalue problem.

Modification of this model to the cavities with cascaded multi-QW active regions or those incorporating the metallized layers is straightforward.

2 Problem formulation and basic equations

Mathematically, the lasing modes can be viewed as source-free solutions to the Maxwell equations. We look for the non-attenuating time-harmonic electromagnetic field $\sim \mathrm{e}^{-ikct}$,

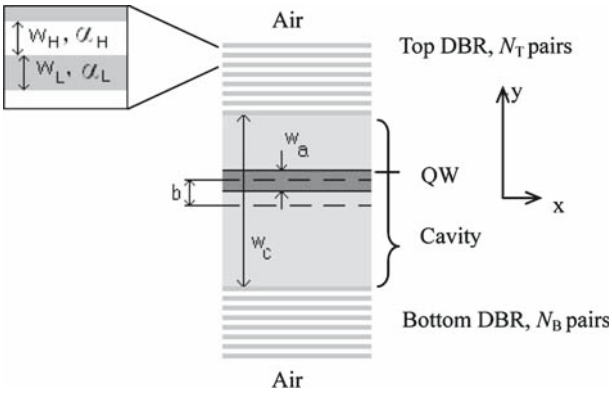

Fig. 1 Sketch of the VCSEL-type layered structure

where $k = \mathrm{Re}\, k > 0$ and c is the light velocity, inside and outside a multilayer dielectric medium schematically depicted in Fig. 1. It consists of the cavity whose width is w_c, sandwiched between two DBRs made of N_T and N_B pairs of high and low-index layers whose thicknesses are w_H and w_L, respectively. Inside the cavity a QW sits of the width w_a.

As we assume that the electromagnetic field does not vary along the axes x and z, it can be characterized by a scalar function E, which is the E_z field component. Off the layer interfaces, this function must satisfy the Helmholtz equation, $[\Delta + k^2 \nu^2(y)]E(y) = 0$. Here, step-like function $\nu(y)$ is assumed 1 outside the cavity and DBRs, i.e., in the lower and upper half-spaces filled with air; inside the layered structure it takes the values corresponding to the refractive indices of semiconductor cavity, α_c, and the high and low-index materials of the DBR pairs, α_H and α_L. All $\alpha_s (s = c, H, L)$ are assumed real, i.e., we neglect the absorption. Following (Smotrova and Nosich 2004; Smotrova et al. 2005), we will assume that $\nu = \alpha_c - \mathrm{i}\gamma$ is complex-valued with a negative imaginary part inside the QW region that corresponds to the active material. The optical field tangential components must satisfy the continuity conditions at the layer interfaces and obey the outgoing wave radiation condition at infinity ($|y| \to \infty$). Keeping in mind source-free solutions to this boundary-value problem, we seek its eigenvalues as a discrete set of pairs of real-valued parameters, (κ_n, γ_n). The first of them is the normalized frequency of lasing, $\kappa = k w_c$ and the second is the associated threshold material gain. Note that the gain per unit length, frequently met in the Fabry-Perot cavities descriptions, is obtained as $g = k\gamma$. This formulation is different from the "classical" formulation of the eigenvalue problem for an open cavity with the complex-valued frequency k being eigenvalue parameter. Note that LEP is still a linear problem, however takes into account the presence of the active region and enables one to extract the thresholds, in terms of γ, in addition to the natural-mode wavelengths. This is more adequate to the lasing than determining the Q-factors ($Q_n = |\mathrm{Re}\, k_n / \mathrm{Im}\, k_n|$) and can be qualified as building a "warm" model of laser. Such a model was systematically introduced in Smotrova and Nosich (2004) and in greater details in Smotrova et al. (2005), although similar ideas have been also expressed elsewhere (e.g., in Klein et al. 1998; Noble et al. 1998; Campenhout et al. 2005).

For a generic DBR-based microcavity with a QW shifted by arbitrary distance b from the centre, our 1D LEP can be reduced to the following equation:

$$\mathrm{e}^{-\mathrm{i}2\kappa(\alpha_c-\mathrm{i}\gamma)(w_a/w_c)} = R_1 R_2, \quad R_{1,2} = \frac{R_{B,T}\mathrm{e}^{\mathrm{i}\kappa\alpha_c[1\pm(2b\mp w_a)/w_c]} + R_a}{1 + \mathrm{e}^{\mathrm{i}\kappa\alpha_c[1\pm(2b\mp w_a)/w_c]} R_{B,T} R_a},$$
$$R_a = \frac{\mathrm{i}\gamma}{2\alpha - \mathrm{i}\gamma}, \tag{1}$$

where $R_{B,T}$ are the Fresnel reflection coefficients of the bottom and top DBR, respectively.

If a lossless cavity with a symmetrically embedded QW ($b = 0$) is sandwiched between two identical DBRs ($R_B = R_T = R_0$) opening into free space, then $R_1 = R_2 = R$ and (1) splits to two independent equations for the symmetric and anti-symmetric modes, respectively:

$$\mathrm{e}^{-\mathrm{i}\kappa(\alpha_c-\mathrm{i}\gamma)(w_a/w_c)} \pm R = 0, \quad R = \frac{R_0\mathrm{e}^{\mathrm{i}\kappa\alpha_c(1-w_a/w_c)} + R_a}{1 + \mathrm{e}^{\mathrm{i}\kappa\alpha_c(1-w_a/w_c)} R_0 R_a}, \tag{2}$$

We emphasize that the LEP and Q-factor problems cannot be reduced to each other by transformations and changes of variables. To establish a link between them, one should be reminded that in the latter case each complex-valued eigenfrequency, $k_n = \mathrm{Re}\, k_n(\gamma) + \mathrm{i}\mathrm{Im}\, k_n(\gamma)$, is a continuous function of the parameter γ. Hence, one can look for a specific value, γ_n, that brings $\mathrm{Im}\, k_n(\gamma)$ to zero, and consider this as the threshold of lasing—this approach was adopted in (Klein et al. 1998; Noble et al. 1998).

Note that looking for a mode Q-factor in a cavity with an active region (like in Ripoll et al. 2004) makes little sense, because it may become arbitrarily large depending on the nearness of the gain γ to the threshold value, at which the Q-factor is infinite. This circumstance cannot be eliminated so far as we assume the harmonic time dependence and neglect nonlinear saturation. Still (Ripoll et al. 2004) is important as it shows how material gain, γ, can be expressed, by using the two-level model, via the parameters of charge carriers and the pump power.

3 Lasing spectra and thresholds for the simplest cavity

To demonstrate the potentials of the LEP analysis, consider first one of the simplest configurations—a dielectric slab in free space (no DBRs), with a symmetric QW of varying width inside the slab. In this case, we can use (2) and put $R_0 = (\alpha_c - 1)/(\alpha_c + 1)$. We have computed the dependences of the lasing frequencies and thresholds on the width of the QW inside the cavity by solving (2) numerically. Here, we apply the two-parameter Newton method presented in (Smotrova et al. 2005) to find the roots in terms of (κ_n, γ_n). These results are shown in Figs. 2 and 3.

Asymptotically, i.e., for $n \gg 1$, the roots of characteristic Eq. 2 behave as $\kappa_n = \pi(n+1)/\alpha_c$ and $\gamma_n = [\kappa_n(w_a/w_c)]^{-1}\ln[(\alpha_c+1)/(\alpha_c-1)]$. This behaviour is generally visible for the plots in Figs. 2 and 3, where the lasing frequencies remain basically unchanged while the thresholds grow up in inverse proportion to the width of QW. For instance, if the QW width is 1/10 of the cavity width, the threshold of the mode with $n = 10$ is approximately 10 times higher than for the same mode in the uniformly active cavity. The oscillations on the curves correspond to the better or worse overlapping between the active layer and the nth mode E-field pattern.

As another example, we have computed dependences of the lasing thresholds and frequencies on the position of thin QW ($w_a = 0.1w_c$) in the same simplest cavity with respect to its centre, for the modes with $n = 10, 11, 12, 13$. As it is seen in Figs. 4a and 5a, the modal thresholds fall and grow conformably to the location of the QW at the humps and zeros of

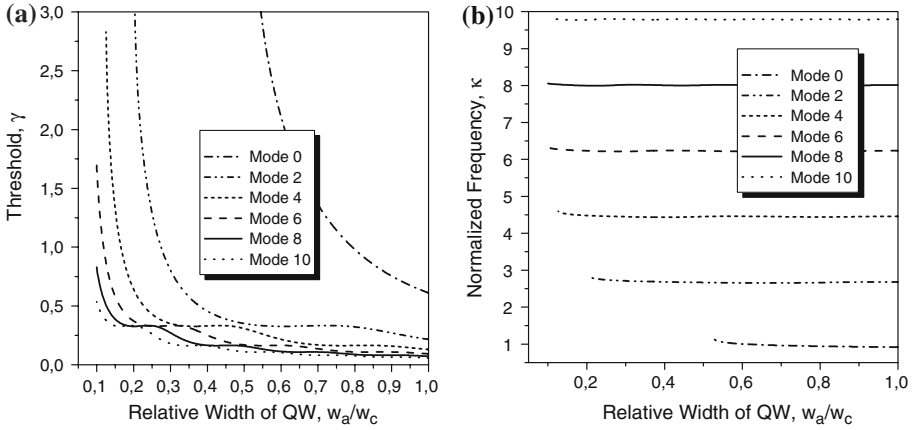

Fig. 2 Dependences of the symmetric mode frequencies (**a**) and thresholds (**b**) on the relative width of the centred QW in a GaAs cavity suspended in the air. The cavity refractive index is 3.53 and modal index is explained in the inset

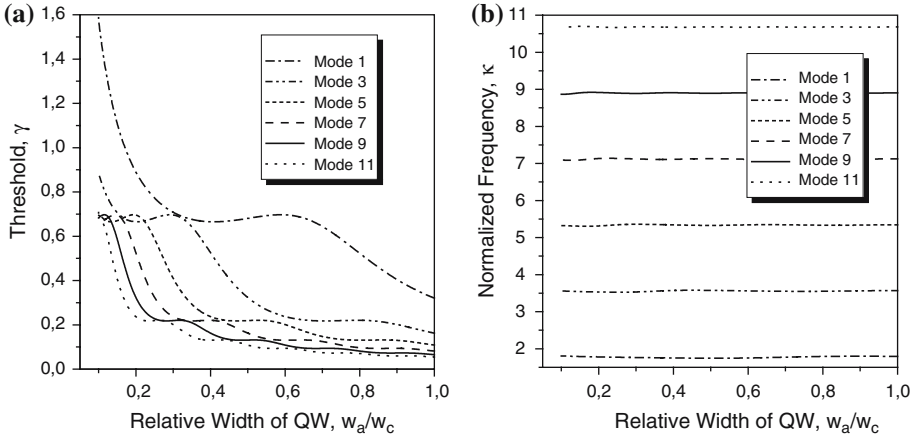

Fig. 3 The same as in Fig. 2 but for the antisymmetric modes

the modal E-field absolute value in the cavity. The frequencies vary in similar oscillating manner however within less than 1% margin around the mean value—see Figs. 4b and 5b.

Note that in Fig. 4 where the even (i.e., having symmetric E-fields with maxima at $y = 0$) modes are presented, placing the QW in the centre of cavity leads to the minimum threshold. While in Fig. 5 where the odd (anti-symmetric E-fields with zeros at $y = 0$) modes are depicted, this results in the maximum threshold. Although such a result may seem obvious, we emphasize that here the modal thresholds are obtained directly and without resorting to the "hot-cavity" nonlinear theories.

Moreover, this is a clear demonstration of the fact that the account of overlapping between the active region and the modal E-field pattern is very elegantly built into the LEP formulation. This is something not tractable within the Q-factor analysis of the passive cavity.

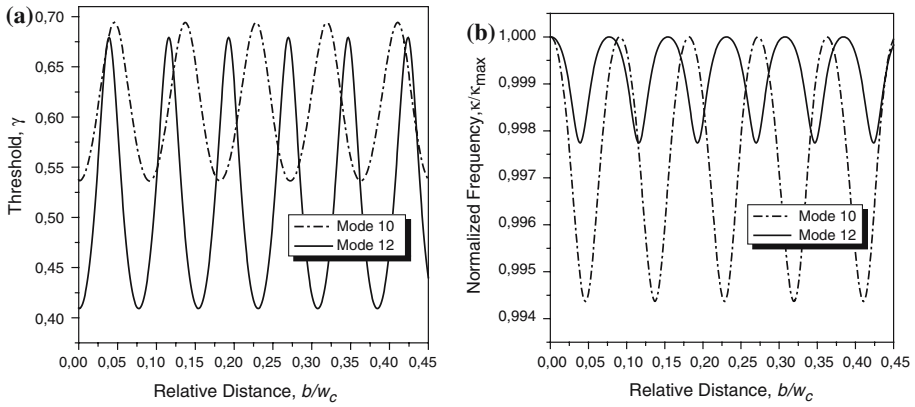

Fig. 4 Dependences of the symmetric mode thresholds (**a**) and frequencies (**b**) on the relative distance between QW and cavity centre. The frequencies are normalized by their maximum values, $\kappa_{10} = 9.82239$ and $\kappa_{12} = 11.59021$

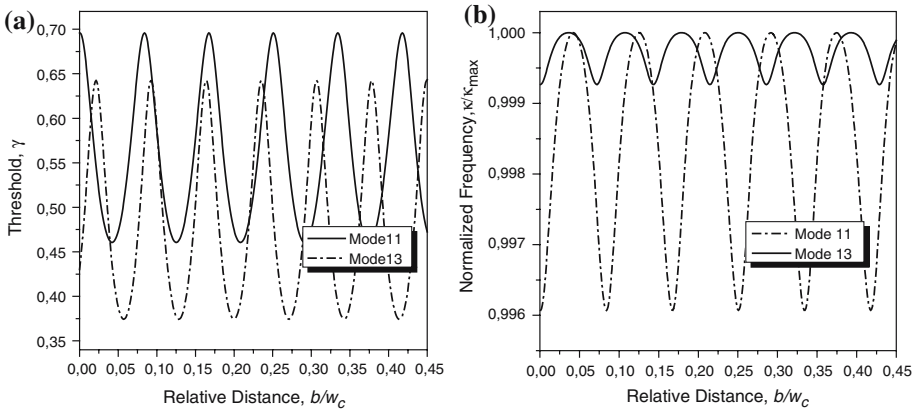

Fig. 5 The same as in Fig. 4 but for the anti-symmetric modes having $\kappa_{11} = 10.70576$ and $\kappa_{13} = 12.47541$

4 DBR treatment with the transfer matrix approach

The goal of this section is to give a brief overview of the solution to the auxiliary problem about the transmission and reflection of the plane wave normally incident at arbitrary multilayer dielectric structure located in free space, as shown in Fig. 6.

Among several equivalent approaches, the transfer matrix method is used most frequently. It originates from the century-old ideas (see Born and Wolf 1968 and references therein); therefore we will not stop on the details here. Some recent refinements of this approach can be found in Kim et al. (1992) and Corzine et al. (1991). The matrix of the transformations of the complex amplitudes of the plane waves normally incident on the first boundary of layers, $\tau(\alpha_0/\alpha_1)$, is introduced as

$$\begin{pmatrix} a_0 \\ b_0 \end{pmatrix} = \tau(\alpha_0/\alpha_1) \begin{pmatrix} a_1 \\ b_1 \end{pmatrix}, \quad \tau(z) = \frac{1}{2} \begin{pmatrix} 1+z & 1-z \\ 1-z & 1+z \end{pmatrix}. \tag{3}$$

The transfer matrix for the whole N-layer structure can is obtained as a product of partial transfer matrices, $\tau(\alpha_i/\alpha_{i+1})$ and diagonal propagation matrices $\Delta(\alpha_i k d_i)$, namely

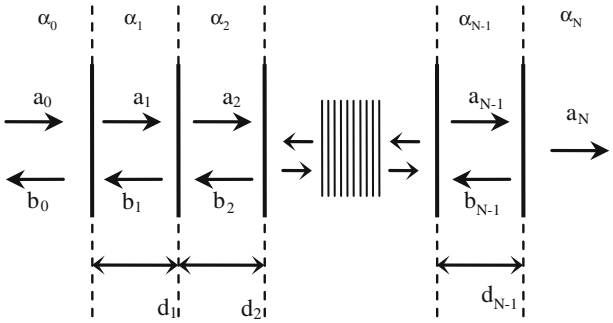

Fig. 6 Multilayer structure for the auxiliary problem

$$P=\begin{pmatrix} p_{11} & p_{12} \\ p_{21} & p_{22} \end{pmatrix}=\tau(\alpha_0/\alpha_1)\cdot\prod_{i=1}^{N-1}\Delta(\alpha_i k d_i)\cdot\tau(\alpha_i/\alpha_{i+1}),\quad \Delta(x)=\frac{1}{2}\begin{pmatrix} \mathrm{e}^{-\mathrm{i}x} & 0 \\ 0 & \mathrm{e}^{\mathrm{i}x} \end{pmatrix} \tag{4}$$

This is the matrix linking together the waves outside of the layered structure as

$$\begin{pmatrix} a_0 \\ b_0 \end{pmatrix} = P\begin{pmatrix} a_N \\ 0 \end{pmatrix} \tag{5}$$

Therefore the reflection and transmission coefficients are given by

$$R = b_0/a_0 = p_{21}/p_{11},\quad T = a_N/a_0 = 1/p_{11}. \tag{6}$$

To illustrate this approach, consider a layered DBR structure consisting of pairs of GaAs and $Ga_{0.8}Al_{0.2}As$ layers having refractive indices $\alpha_H = 3.53$ and $\alpha_L = 3.08$, respectively. Assuming that this structure is immersed into air, we may compute the reflection coefficient of the incident plane wave by using (3)–(6). Note that conservation of energy demands that $|R|^2 + |T|^2 = 1$.

The results are shown in Fig. 7. They demonstrate, as expected, that the DBR has a number of rejection frequency bands, whose locations and widths are determined by the composition

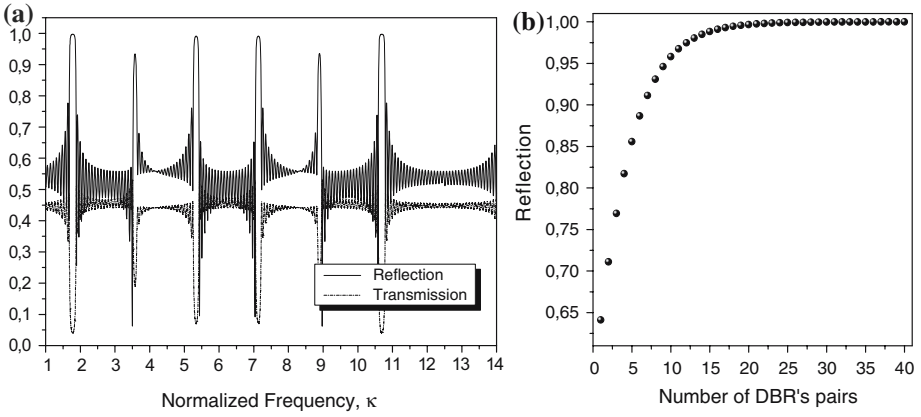

Fig. 7 Reflection coefficient $|R|$ versus the normalized frequency for DBR consisting of 20 pairs of layers, $w_H/w_L = 1.16$ (**a**) and the same value versus the number of pairs of quarter-wavelength-width layers for the normalized frequency $\kappa = 10.67$ (**b**)

of DBR pairs—see Fig. 7a. Note the presence of such a band around the normalized frequency $\kappa = 10.67$. Inside the rejection band, the transmission coefficient exponentially decreases with increasing the number of DBR pairs that leads to the corresponding growth of reflection coefficient—see Fig. 7b. For example, this value for the DBR having 40 pairs of layers equals to 0.99998.

5 Effect of DBR on the lasing thresholds and frequencies

Now we may come back to the lasing in a layered microcavity equipped with an active region and see how the use of DBR effects the thresholds and frequencies of lasing modes. This means that we will study the LEP for the corresponding configuration. Consider a cavity with the centred QW active region having the width w_a of 1/10 of the cavity one, w_c, and placed between two identical DBRs opening into the air. Material composition of the DBRs is the same as in the previous section; the cavity is of GaAs ($\alpha_c = 3.53$), and the complex-valued index of the QW is assumed to be $\nu = 3.53 - \mathrm{i}\gamma$, where γ is eigenvalue. We apply the transfer-matrix method to calculate the DBR reflectivities and the two-parameter Newton method mentioned above to find the roots of (2) in terms of (κ_n, γ_n). These results are shown in Figs. 8a–d as points on the (κ, γ) plane.

For the modes, whose frequencies happen to get into the DBR rejection bands, one can see the lowering of the thresholds. For example, this is obvious for the mode $n = 11$ in Fig. 8a, whose normalized frequency is approximately $\kappa_{11} = 10.67$ (compare to the frequency scan of R in Fig. 7a for a single DBR mirror of the same composition).

However the thresholds of the neighbouring modes, which lay off the rejection band of DBRs, do not feel their presence or can even get higher than the same values for the "bare" cavity (i.e., without DBRs). This can be explained by the effect of the pulling of the E-field into the DBRs and by the corresponding worthening of the overlap between the modal E-field of the thin QW active region.

Table 1 contains precise values of the lasing frequencies and thresholds of the lowest-threshold modes in each of the (a) to (d) sub-figures of Fig. 8.

If a cavity mode has the frequency lying inside of a DBR rejection band, its threshold decreases exponentially to the value determined by the number of DBR pairs (Fig. 9a), while the frequency variation is very small as it is well seen in Fig. 9b.

Table 1 Minimum-threshold mode characteristics for the OW-equipped cavities with DBR compositions presented in Figs. 8a–d

(a) $w_H = 79.63$, $w_L = 69.49$		(b) $w_H = 112.6$, $w_L = 27.9$		(c) $w_H = 93$, $w_L = 46.5$		(d) $w_H = 69.75$, $w_L = 69.75$	
$n = 11$	$\kappa = 10.67964$	$n = 6$	$\kappa = 6.22957$	$n = 10$	$\kappa = 9.78965$	$n = 5$	$\kappa = 5.33983$
	$\gamma = 0.00771$		$\gamma = 0.07291$		$\gamma = 0.01544$		$\gamma = 0.02537$
				$n = 15$	$\kappa = 14.23951$	$n = 6$	$\kappa = 6.22978$
					$\gamma = 0.00498$		$\gamma = 0.0152$

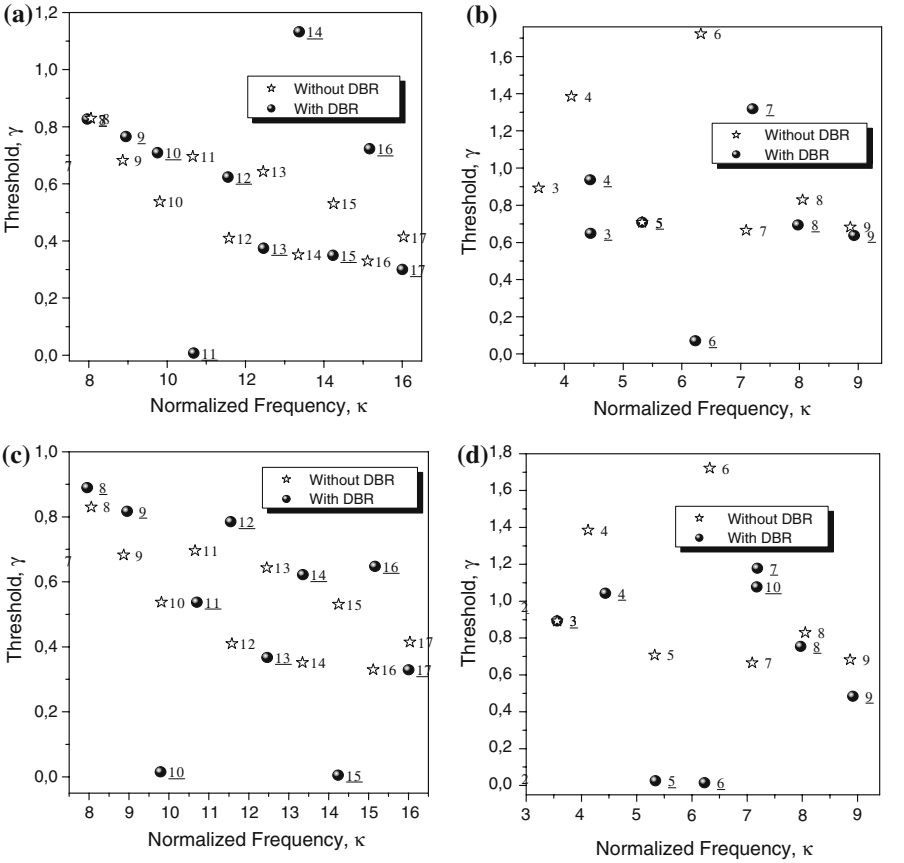

Fig. 8 Effect of DBRs with different layer thicknesses on the lasing frequencies and thresholds in a GaAs cavity with symmetric QW (all dimensions are in nanometers): (**a**) $w_H = 79.63$, $w_L = 69.48$, (**b**) $w_H = 112.6$, $w_L = 27.9$, (**c**) $w_H = 93$, $w_L = 46.5$, (**d**) $w_H = 69.75$, $w_L = 69.75$. QW width is $w_a = 0.1w_c$, number of DBR pairs is $N = 20$ Modal indices are marked with numbers

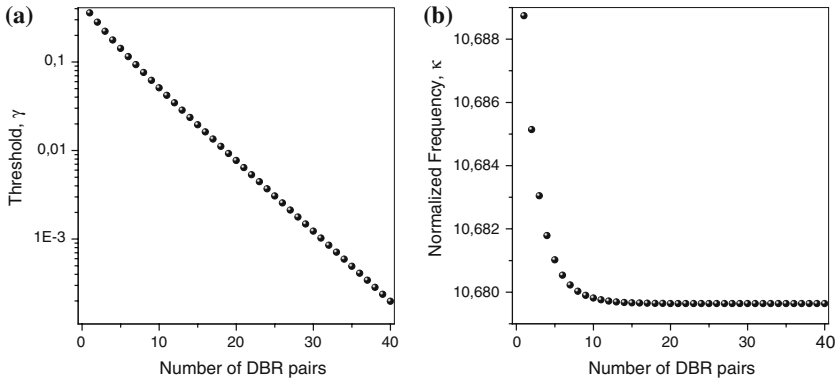

Fig. 9 Dependences of the lasing threshold (**a**) and the normalized frequency t (**b**) for the mode with $n = 11$ on the number of layer pairs in the DBRs corresponding to Fig. 8a with a GaAs cavity and centered active region of $w_a = 0.1w_c$

6 Conclusions

We have studied the novel 1D lasing eigenvalue problem for the modes in a VCSEL-type layered dielectric structure containing a cavity, a QW active region, and two DBRs opening into the air. The characteristic equation has been derived using the Helmholtz equation with outgoing radiation condition below and above the layers and the transfer-matrix method. Numerical solutions have been obtained, in particular, for the symmetric and antisymmetric lasing modes in the symmetrical geometry with the centred QW occupying 1/10 of the cavity and two identical DBRs. Computations have shown that the modes, whose frequencies in stand-alone cavity happen to lay in the rejection bands of the DBRs, obtain lower thresholds when placed between the reflectors. Here, the mode frequency weakly depends on the number of pairs of layers in DBR however the threshold goes down exponentially. The novelty of our study lies in the direct quantification of lasing thresholds instead of the previously studied Q-factors of passive cavity modes. This is achieved by using a specifically tailored electromagnetic eigenvalue problem, i.e., the LEP, with exact boundary and radiation conditions.

This approach can be easily adapted to arbitrarily-layered lasing geometries, e.g., cavities with multiple QWs, additional substrates and superstrates, noble-metal claddings, etc. The considered layered geometry can be further employed as a model of the host medium for periodically structured active regions, which are actively investigated today.

Acknowledgements We are grateful to Ms. Elena Smotrova for stimulating discussions and aid in computations and to Prof. Trevor Benson and Prof. Phillip Sewell for encouragement. This work was supported in part by the National Academy of Sciences of Ukraine via project PORIG #36/07H. The first author was also supported by the IEEE AP-S Graduate Student Fellowship.

References

Born, M., Wolf, E.: Principles of Optics, 4th ed. Pergamon Press, Oxford (1968)

Campenhout, J.V., Bienstman, P., Baets, R.: Band-edge lasing in gold-clad photonic-crystal membranes. IEEE J. Commun. **23**(7), 1418–1423 (2005)

Chung, I.-S., Lee, Y.T., Kim , J.E., Park, H.Y.: Effect of outermost layers on resonant cavity enhanced devices. J. Appl. Phys. **96**(05), 2423–2427 (2004)

Corzine, S.W. et al.: A tanh substitution technique for the analysis of abrupt and graded interface multilayer dielectric stacks. IEEE J. Quant. Electron. **27**, 2086 (1991)

De Leonardis, F., Passaro, V.M.N., Magno, F.: Improved simulation of VCSEL distributed Bragg reflectors. J. Comput. Electron. **6**, 289–292 (2007)

Huffaker, D.L., Deppe, D.G.: Low-threshold VCSELs based on high-contrast distributed Bragg reflectors. Appl. Phys. Lett. **70**(14), 1781–1783 (1997)

Kim, B.G. et al.: Comparison between the matrix method and the coupled-wave method in the analysis of Bragg reflector structures. J. Opt. Soc. Am. **9**, 132 (1992)

Klein, B., Register, L.F., Hess, K., Deppe, D.G., Deng, Q.: Self-consistent Green's function approach to the analysis of dielectrically apertured VCSELs. Appl. Phys. Lett. **73**(23), 3324–3326 (1998)

Noble, M.J., Loehr, J.P., Lott, J.A.: Analysis of microcavity VCSEL lasing modes using a full-vector weighted index method. IEEE J. Quantum Electron. **34**, 1890–1903 (1998)

Piprek, J. (ed.): Optoelectronic Devices: Advanced Simulation and Analysis. Springer, Berlin (2005)

Ripoll, J., Soukoulis, C.M., Economou, E.N.: Optimal tuning of lasing modes through collective particle resonance. J. Opt. Soc. Am. B. **21**(1), 141–149 (2004)

Smotrova, E.I., Nosich, A.I.: Mathematical analysis of the lasing eigenvalue problem for the whispering-gallery modes in a 2-D circular dielectric microcavity. Opt. Quant. Electron. **36**(1–3), 213–221 (2004)

Smotrova, E.I., Nosich, A.I., Benson, T.M., Sewell, P.: Cold-cavity thresholds of microdisks with uniform and non-uniform gain: quasi-3D modelling with accurate 2D analysis. IEEE J. Quant. Electron. **11**(5), 1135–1142 (2005)

Streiff, M., Witzig, A., Pfeiffer, M., Royo, P., Fichtner, W.: A comprehensive VCSEL device simulator. IEEE J. Quantum Elect. **9**(3), 879–891 (2003)

Yang, G.M., MacDougal, M.H., Zhao, H., Dapkus, P.D.: Microcavity effects on the spontaneous emission from InGaAdGaAs quantum wells. J. Appl. Phys. **78**(6), 3605–3609 (1995)

Yu, S.F.: Analysis and Design of Vertical Cavity Surface Emitting Lasers. Wiley (2003)

Zhang, X.H., Chua, S.J., Liu, W., Wang, L.S., Yong, A.M., Chou, S.Y.: Crack-free fully epitaxial nitride microcavity with AlGaN/GaN distributed Bragg reflectors and InGaN/GaN quantum wells. Appl. Phys. Lett. **88**, 191111 (2006)